

A non-linear orthotropic binary model to predict thermo-mechanical behaviour of plain weave ceramic matrix composites

Mingming Chen¹, Heyin Qi², Shutong Cheng³, Daxu Zhang^{4*}, and Jinghai Gong⁵

¹ School of Naval Architecture, Ocean and civil Engineering, Shanghai Jiao Tong University, Shanghai 200240, China

² School of Naval Architecture, Ocean and civil Engineering, Shanghai Jiao Tong University, Shanghai 200240, China

³ School of Naval Architecture, Ocean and civil Engineering, Shanghai Jiao Tong University, Shanghai 200240, China, E-mail: daxu.zhang@sjtu.edu.cn,
http://naoce.sjtu.edu.cn/en/teachershow.aspx?info_lb=22&info_id=280&flag=2

⁴ School of Naval Architecture, Ocean and civil Engineering, Shanghai Jiao Tong University, Shanghai 200240, China

⁵ School of Naval Architecture, Ocean and civil Engineering, Shanghai Jiao Tong University, Shanghai 200240, China

Keywords: Ceramic matrix composites, Textile composites, Orthotropic properties, Thermal conductivity, Thermo-mechanical behaviour

ABSTRACT

This paper addresses the development of a coupled thermal-stress finite element model based on the previous work, stress-displacement model using non-linear orthotropic constitutive properties. The Binary Model utilises two virtual components that comprise the composite tow: (i) a 1-D tow element; and, (ii) a 3-D effective medium element to represent the fibre-dominated and the matrix-dominated properties, respectively. The coupled thermal-stress model was formulated using the mechanical properties and strain dependent thermal properties. The non-linear multi-axial thermal conductivity-strain curves have been discretised by multi-linear curves. The finite element package Abaqus with a user-defined subroutine USDFLD was used to implement the simulations. The effects of waviness on composite stress-strain response and thermal conductivity-strain curve have been made. The numerical results have been validated by the comparison of predictions with the experimental data, and good agreement has been achieved. For the DLR-XT plain weave laminate, the dominant mechanism of thermal conductivity degradation is combined wake debonding and out-of-plane shear failure.

1 INTRODUCTION

Ceramic matrix composites (CMCs) possess the characters of low density, high modulus and good thermal stability; they have great potential in hot structures, such as rocket nozzles, combustor liners of turbine engines, space shuttle thermal protection systems, and nuclear fuel cladding tubes. ([1-3]). Compared to metallic alloys, the key material property is the strength-to-weight ratio in the temperature range of 1000-1600 °C. In service environments, CMC components may experience the complex and harsh thermo-mechanical loadings. Their fracture strengths at high temperatures are the crucial factors to the design and safety of such high temperature structural materials. Therefore, it necessitates the development of an accurate yet highly computational efficient model, which is capable of predicting thermo-mechanical behaviour of CMC components requiring a long service life.

Over the past decades, numerous efforts have been made to investigate the thermal behaviour of CMCs. Sheikh et al [4] have presented a complex weave model of a plain weave CMC. Their model is three-dimensional, and is a step towards the thermal finite-element modelling of complex composite architecture. Their research included the effects of directionality in thermal transport by the

introduction of the individual properties of fibre tows and matrix/medium materials. This level of understanding was further advanced by Del Puglia et al [5-7] for the same DLR-XT material. In many applications, e.g. high temperature heat pipe used to contain pressurised fluids that often undergo heat transfer, are more often subjected to thermo-mechanical loadings. However the very strong coupling between mechanical behaviour and thermal properties is recently not well understood ([8]). The greatest challenge associated with the correct analysis is the degradation of the mechanical and thermal properties with composite strain due to internal damage; hence the complex damage mechanisms of CMCs under thermo-mechanical loadings can be activated. These requirements would necessitate precise descriptions of constitutive models, and the ability to predict the mechanical and thermal responses at the design stage.

Generally, existing approaches for analyzing the thermo-mechanical coupling can be categorized into two types: direct and indirect. Direct methods are used to solve the temperature and stress fields simultaneously while indirect methods are appropriate for the case of weak coupled temperature and stress fields. In the case of indirect methods, such as that of Liu et al [9], in which a sequential coupling finite element algorithm was derived for heat pipe cooled thermal protection structure by introducing penalty functions. Nevertheless, indirect methods require a quite large number of equations especially in the case of complex thermo-mechanical coupling problems, leading to high computational costs.

The paper addresses the development of a coupled thermal-stress finite element model based on the previous work, i.e. stress-displacement model using non-linear orthotropic constitutive properties. This work relies on a good understanding of damage mechanisms as well as constitutive laws for the constituent materials, including elasticity and thermal properties. The layout of the paper is as follows. First, the damage mechanisms under thermo-mechanical loadings will be introduced. Secondly the Binary Model and its non-linear constitutive equations employed are described. Then, the test data of the 10 high carbon fibre/amorphous carbon matrix-SiC matrix (C/C-SiC) DLR-XT plain weave laminates will be used to validate the predictions. Also, the effects of waviness and shear failure will be investigated on composite stress-strain response and thermal conductivity-strain curve.

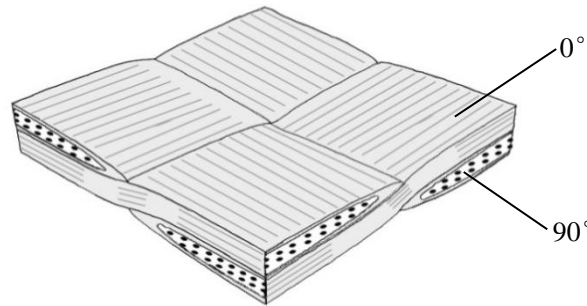


Figure 1: Schematic drawings of unit cells for DLR-XT material, showing an assemblage of four tows.

2 DAMAGE MECHANISMS UNDER THERMO-MECHANICAL LOADINGS

2.1 Tow longitudinal thermal conductivity

Tang et al [10] have proposed that longitudinal thermal conductivity is controlled by the air gaps introduced on matrix cracking, with regular crack separation distance and fibre failure. They have derived equations, based on the thermo-mechanical properties of the constituent materials, which can be numerically integrated to produce variations of the local tow longitudinal thermal conductivity, k_{Long}^{ℓ} , with local tow strain, ε_{11}^{ℓ} .

For the DLR-XT material, an initial value of $k_{Long}^{Initial} = k_{11}^{\ell} = 20.38 \text{ Wm}^{-1}\text{K}^{-1}$ has been determined using the constituent materials data. Fig.2a has been discretised as multi-linear curves using typically 25 data points. The first step reduction in k_{Long}^{ℓ} shown in Fig.2a is due to matrix cracking and the subsequent monotonic decrease that results from fibre failure. The data in Fig.2a is used as the discretised multi-linear materials input data for the finite element model.

2.2 Tow transverse thermal conductivity

Tang et al [10] have indicated that the degradation of transverse thermal conductivity is controlled by the process of wake debonding which produces a cylindrical air gap at the interface between fibre and matrix a block of material associated with a single located between two adjacent matrix as shown in Fig.11 of Blacklock and Hayhurst [11]. The poor transverse thermal conductivity of the cylindrical air gap prevents transverse heat flow through the fibre and some of the matrix. For DLR-XT an initial value of $k_{Tran}^{Initial} = k_{22}^{\ell} = k_{33}^{\ell} = 12.56 \text{ Wm}^{-1}\text{K}^{-1}$, has been obtained using data from Tables A1 and A2 of Tang et al [12]. The degradation of k_{Tran}^{ℓ} against ε_{11}^{ℓ} for DLR-XT is given in Fig.2b, which again are used as the multi-linear input data for the finite element model. The mechanism of transverse tow thermal conductivity is combined wake debonding and fibre failure as modelled by Tang et al [10].

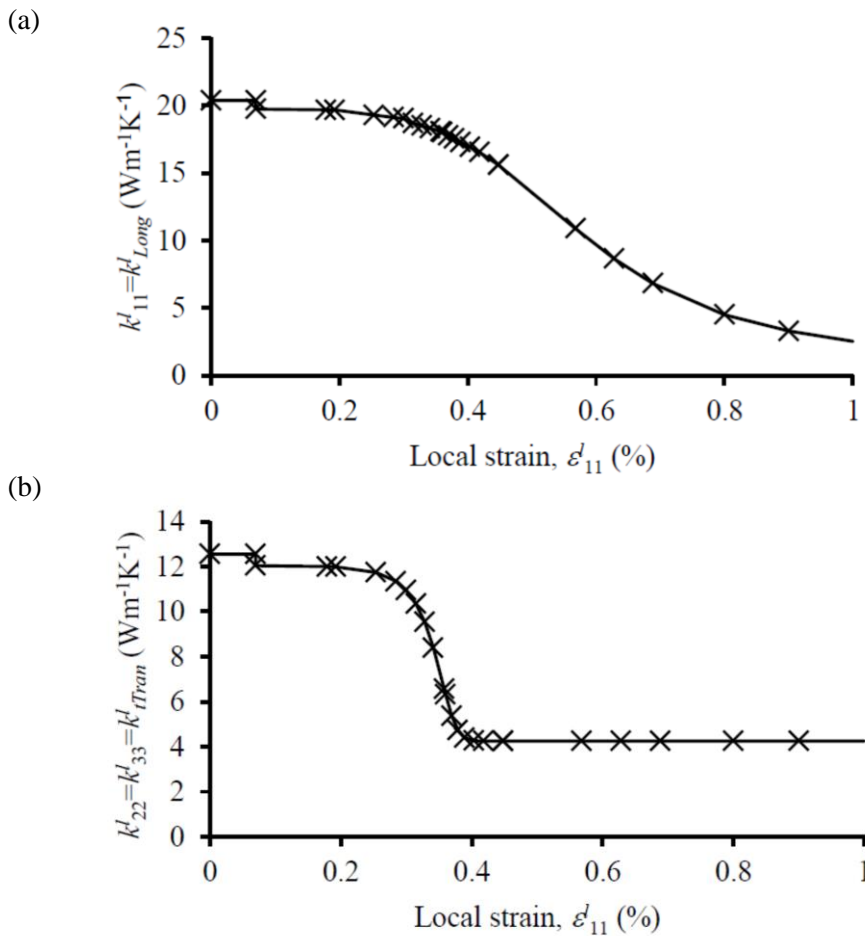


Figure 2: Thermal material properties of uni-directional DLR-XT tow (a) longitudinal thermal conductivity-strain curve; (b) transverse thermal conductivity-strain curve.

2 FORMULATION OF THE BINARY MODEL

The Binary Model was introduced as a computationally high efficient and comprehensive adaptable approach for the analysis of textile composites, including 3D weaves and braids, knitted fabrics, etc (Cox et al [13]). In its original formulation, due to the highly anisotropic and heterogeneous characteristics, a 3-D composite is divided into two virtual components: 1-D tow element represents the axial properties of fibre tows, and 3-D solid effective medium element represents the transverse stiffness, shear stiffness and Poisson's effects of fibre tows. The tow elements and effective medium elements are coupled by embedded displacement constraints. The Binary Model technique allows tow

elements and effective medium elements to be modelled respectively; and, this greatly simplifies mesh generation. Early work (Yang and Cox [14-15]; Blacklock and Hayhurst [16]) has demonstrated that the Binary Model can give an accurate prediction of the global axial stiffness of complex 3-D textiles. For these reasons it is the chosen analysis technique for the research reported herein.

2.2 Constitutive laws for effective medium and tow elements of the Binary Model

Due to the reinforcement of continuous fibre bundles, CMC tows exhibit significantly different longitudinal and transverse non-linear behaviour. The constituent material properties used in the Binary Model, due to the interactions of orthogonal 1-D tow elements, need to be judiciously assigned. The longitudinal medium stiffness could be deliberately set equal to the transverse medium stiffness, i.e. an isotropic medium material. However, an orthotropic medium rather than isotropic medium is believed to be more appropriate. Since it is only in this way, that the degradation of material properties in different directions can be taken into account.

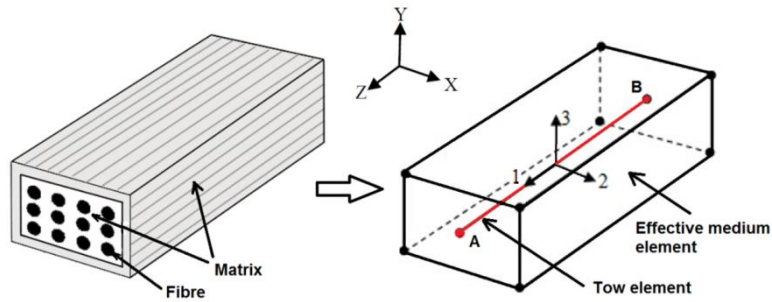


Figure 3: Principle of Binary Model: one tow element AB embedded in one 8-noded effective medium element.

Constitutive laws for effective medium and tow elements are presented in this section in terms of **non-linear orthotropic** material properties of a uni-directional tow. As illustrated in Fig. 3 for the local coordinate system, the 1-axis is aligned with the fibre direction, the 2-axis is perpendicular to the fibre in the plane of the layer, and the 3-axis is perpendicular to the plane of the layer. The global coordinate system of the unit cell model is (x, y, z).

The orthotropic constitutive properties that are consistent with the micromechanics of matrix cracking were assigned to the effective medium elements. Effective medium elements, which represent matrix-dominated contributions to stiffness, were assumed to be **orthotropic** with nine independent material properties, Young's moduli: E_1^{EM} , E_2^{EM} and E_3^{EM} ; Poisson's ratios: ν_{12}^{EM} , ν_{13}^{EM} and ν_{23}^{EM} ; Shear moduli: G_{12}^{EM} , G_{13}^{EM} , and G_{23}^{EM} , given by

$$E_2^{EM} = E_3^{EM} = E_x^{UD} \quad (1)$$

$$\nu_{12}^{EM} = \nu_{13}^{EM} = \nu_{zx}^{UD}; \quad \nu_{23}^{EM} = \nu_{xy}^{UD} \quad (2)$$

$$G_{12}^{EM} = G_{13}^{EM} = G_{zx}^{UD}; \quad G_{23}^{EM} = G_{xy}^{UD} \quad (3)$$

where the superscripts, *EM* and *UD*, denote effective medium and uni-directional tows, respectively. Effective medium can be modelled by continuum elements, and 8-node linear bricks were used in the current work.

The tow elements represent the fibre-dominated properties, and therefore were assumed to have only axial stiffness. Such that the overall uni-directional axial stiffness in the local 1-direction is $k_1^{UD} = k_1^{Tow} + k_1^{EM}$. Hence, according to the stiffness equivalent substitution principle, the axial stiffness of the tow elements can be expressed by

$$k_1^{Tow} = k_1^{UD} - k_1^{EM} = (E_1^{UD} - E_1^{EM}) \times A \quad (4)$$

where *A* denotes the cross-sectional area of a tow. The tow elements were modelled by 1-D truss elements within Abaqus.

The constitutive laws for elasticity are presented above; and the constitutive laws for thermal conductivity are addressed in Section 4.1 for detailed.

3.2 Incremental constitutive equations

In the solution of non-linear finite element analysis problem, the non-linear stress-strain response was discretised to a multi-linear curve. The loading was imposed in terms of the displacement boundary condition, i.e. loading was modelled with displacement control rather than force control. The applied displacement was divided into many small increments. In each increment, linear material properties were used in the constitutive equations for both tow element material; and for effective medium/matrix material, be it either an assumed isotropic or orthotropic material. If the numerical solution was acceptable in the current increment, the solution proceeds to the next load increment in order to enable the model to approach an equilibrium state, otherwise the increment is reduced and several iterations were necessary until the convergence can be obtained. The incremental constitutive equations can be expressed by

$$\{\Delta\sigma\} = [C(\Delta\epsilon)]\{\Delta\epsilon\} \quad (5)$$

where $\{\Delta\sigma\}$ is the stress increment vector, $[C(\Delta\epsilon)]$ is the incremental stiffness matrix, and $\{\Delta\epsilon\}$ is the strain increment vector.

Considering the thermal stress caused by temperature gradient, Eq. (5) can be extended to

$$\{\Delta\sigma\} = [C(\Delta\epsilon, \mathbf{t})](\{\Delta\epsilon\} - \{\Delta\epsilon^t\}) \quad (6)$$

where, $\{\epsilon^t\} = [\alpha]\Delta t$, $\{\alpha\} = [\alpha_1 \quad \alpha_2 \quad \alpha_3 \quad 0 \quad 0 \quad 0]^T$

In this paper, the material non-linearity is mainly considered to be activated by degradation of mechanical properties due to strain-induced damage.

3.3 Failure criterion

The failure criteria for effective medium and tow elements were taken to be defined by the maximum principal strain criterion to detect the strain-induced damage. When strain components of effective medium in the principal material direction exceed the critical value associated with cracking, then failure occurs. The composite failure strain is dominated by the tow elements; in physical reality by the local strain $\epsilon_1 > \epsilon_{wd}$, where the material property ϵ_{wd} corresponds to the strain when one half of blocks in a tow ($N/N_T = 0.5$) have failure.

4 FINITE ELEMENT MODEL

This paper addresses the development of a coupled thermal-stress finite element model based on the previous work, i.e. stress-displacement model using non-linear orthotropic constitutive properties. An unit cell of 16 2-node truss elements and 32 8-node hexahedral solid elements was chosen to represent the whole material. The non-linear stress-strain curves were discretised to be multi-linear elastic and Poisson's ratios-strain curves are used. The coupled thermal-stress model employed here was formulated using the strain dependent thermal material properties. The finite element package Abaqus (SIMULIA [17]) with a user-defined subroutine USDFLD was used to implement the simulations. The formulation of mechanical behaviour has been established in the previous work, hence the following mainly introduces the formulation of thermal behaviour of the model.

4.1 Steady-state heat conduction equation

The effective medium is assumed to be thermally orthotropic. For the present three dimensional steady-state heat conduction problem, there are three independent thermal conductivity, k_{11} , k_{22} and k_{33} relative to the local tow axes. For anisotropic continuum, the steady-state heat conduction equation is given by Fourier's law (Fourier [18]):

$$\begin{Bmatrix} q_1 \\ q_2 \\ q_3 \end{Bmatrix} = - \begin{bmatrix} k_{11} & k_{12} & k_{13} \\ k_{21} & k_{22} & k_{23} \\ k_{31} & k_{32} & k_{33} \end{bmatrix} \begin{Bmatrix} \partial T / \partial x_1 \\ \partial T / \partial x_2 \\ \partial T / \partial x_3 \end{Bmatrix} \quad (7)$$

where q_i is the heat flux; k_{ij} is the thermal conductivity; and $\partial T / \partial x_i$ is the thermal gradient ($i, j=1, 2, 3$). Classical thermodynamic theory has manifested that the conductivity tensor k_{ij} is symmetric with $k_{ij} = k_{ji}$, and the coupling terms in the thermal conductivity matrix are zero. Hence, a simplified relation can be derived:

$$\begin{Bmatrix} q_1 \\ q_2 \\ q_3 \end{Bmatrix} = - \begin{bmatrix} k_{11}^\ell & 0 & 0 \\ 0 & k_{22}^\ell & 0 \\ 0 & 0 & k_{33}^\ell \end{bmatrix} \begin{Bmatrix} \partial T / \partial x_1 \\ \partial T / \partial x_2 \\ \partial T / \partial x_3 \end{Bmatrix} \quad (8)$$

where k_{11}^ℓ denotes thermal conductivity along the tow, k_{22}^ℓ denotes the in-plane transverse tow thermal conductivity, k_{33}^ℓ denotes the out-of-plane (through-thickness) transverse tow thermal conductivity in the local coordinates, respectively.

4.2 Boundary condition

In comparison with other numerical models for woven CMCs, e.g. conventional fine-mesh model (Sheikh et al [4]) or homogenised coarse-mesh model (Zhang and Hayhurst [19-21]), the mesh generation for the Binary Model is much more straight forward. The topology of woven tows can be easily captured by fluctuations of 1-D tow elements. The Binary Model employs two mesh systems including 2-node truss elements representing the fibre tows and 8-node solid effective medium elements that define the external geometry and represent the matrix-dominated properties, which facilitates the spatial matching of fibre tows and matrix and obviates the complexity of matrix grids. The two mesh systems are coupled by the multi-point constraints in Abaqus. The dimensions of the DLR-XT unit cell are $1.744 \times 1.744 \times 0.322 \text{ mm}^3$ and its mesh is shown in Fig.4. To simulate a uni-axial straining along the 0° tow direction, a periodic displacement boundary condition was applied to the unit cell. Steady-state heat conduction was modelled by application of a unity thermal gradient between the top and bottom faces of the unit cell, all the other faces were lagged.

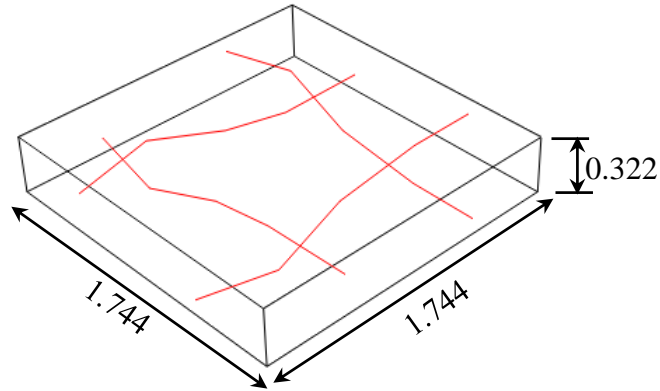


Figure 4: Mesh and geometry of unit cell Binary model of a plain weave DLR-XT (C-C/SiC) material, all dimensions in mm.

4.3 Modelling of waviness

Waviness also exists in woven CMCs, and is frequently more severe than that for conventional laminates. The misalignment angle, ζ , in the DLR-XT material has been measured over a large region of the available micrographs, which are much bigger than the micrograph shown by Sheikh et al [8] and a value of $\zeta = \pm 7^\circ$ has been measured. In this study, the unit cell Binary Models with

$\zeta = 0^\circ$ and $\zeta = \pm 7^\circ$ are employed here.

4.4 Material properties

The longitudinal stress-strain curve of the effective medium is assumed to drop linearly from the peak at the matrix cracking strain of 0.05% to zero at the composite failure strain of 0.38%. The variation with longitudinal strain of the two identical Poisson's ratios, ν_{12}^{EM} and ν_{13}^{EM} can be obtained. The through-thickness and shear stress-strain curves are assumed to be linear elastic until failure. The material properties of tow elements can be calculated from Eq. (4).

5 RESULTS AND DISCUSSION

5.1 Mechanical response

Two predictions are shown in Fig.5: one for zero waviness, $\zeta = 0^\circ$, and the other for a waviness of $\zeta = \pm 7^\circ$. The curve for $\zeta = \pm 7^\circ$ compares well with the experimental data.

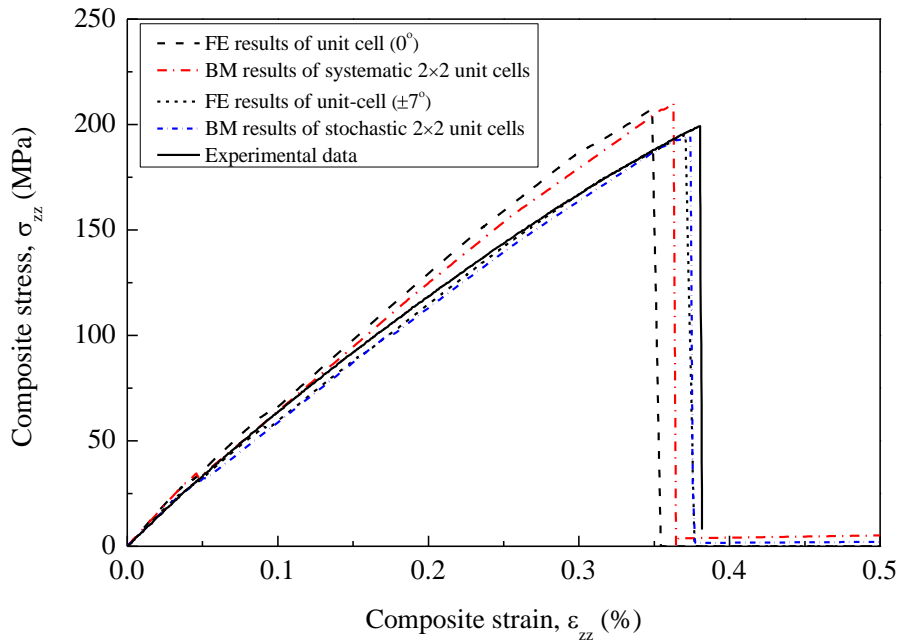


Figure 5: Comparison among the systematic and stochastic Binary Model results, the finite element results (Zhang and Hayhurst [19-21]) and experimental data (Sheikh et al [8]) for a plain weave DLR-XT laminate.

5.2 Thermal response

For the material tested by Sheikh et al [8], no results were obtained for in-plane composite thermal conductivity. Hence, the attempt has been made to predict in-plane thermal conductivity. Predictions of the variation of composite transverse thermal conductivity, k_{33} , with composite strain, $(\varepsilon_{11})_\infty$ without considering the effects of shear strain failure described in Section 2.3. Figs.6 shows a comparison between Binary Model results; more conventional FE results of Zhang and Hayhurst [19-21]; and the experimental data of Sheikh et al [8]. It can be seen from these figures, excellent results have been achieved. Therefore, the proposed constitutive models and the computational capability of the Binary Model can be demonstrated, but the results of experimental 2 will be given a low priority due to the excessive scatter on the data. The reason for this scatter is unknown.

Two predictions without considering the effects of shear failure can be obtained, the curve for waviness of $\zeta = 0^\circ$ compares well with the experimental data. The curve for $\zeta = \pm 7^\circ$, Fig.6, starts to deviate from the experimental data at the strain $(\varepsilon_{11})_\infty \approx 0.19\%$, and the error increases. However the composite possesses waviness of $\zeta = \pm 7^\circ$, the model for $\zeta = 0^\circ$ is not appropriate. The same conclusions have been drawn in Zhang and Hayhurst [20].

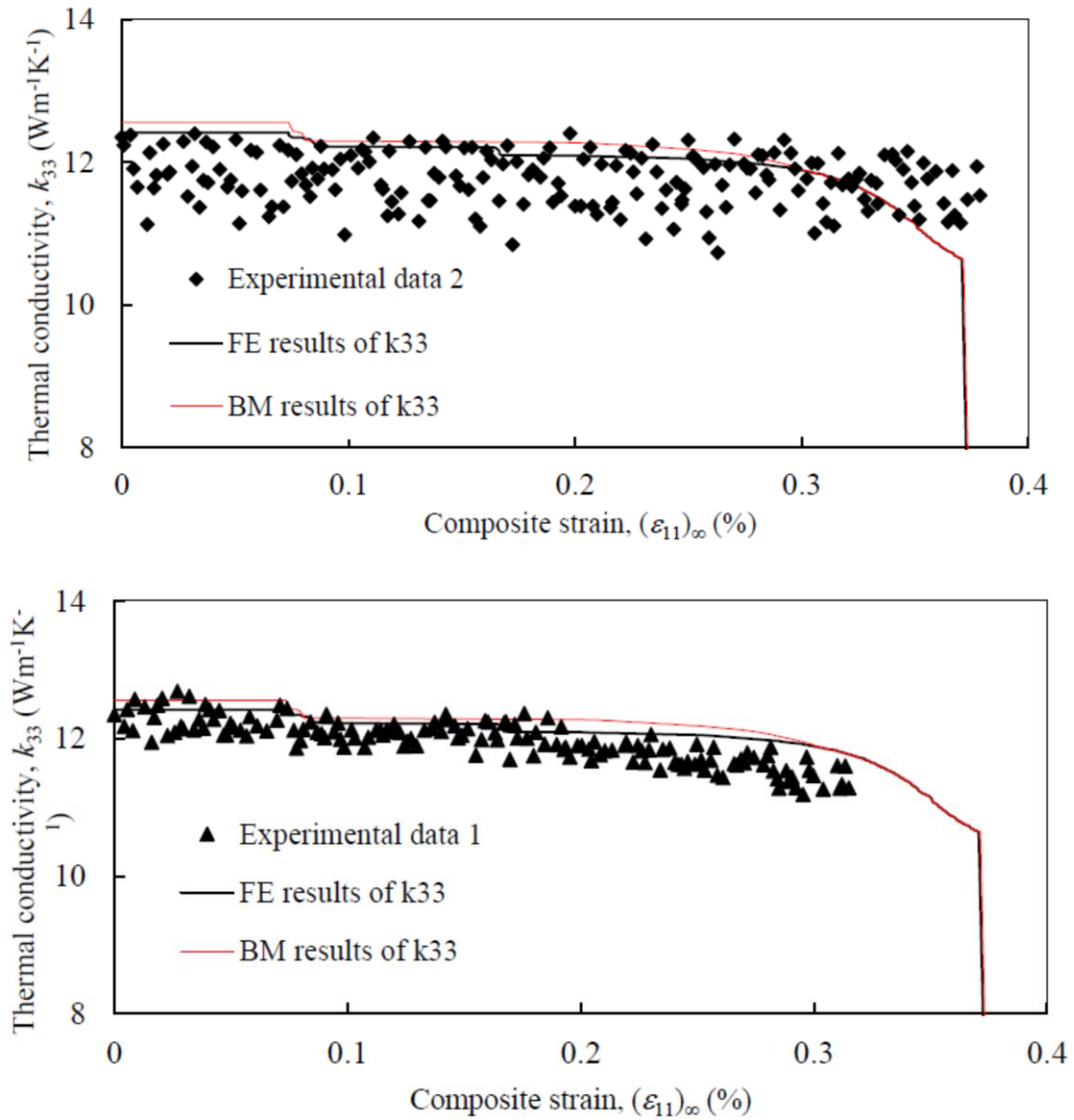


Figure 6: Predicted through-thickness thermal conductivities for DLR-XT ($\zeta = \pm 7^\circ$) with no effects of shear failure.

6 CONCLUSIONS

(1) The non-linear orthotropic Binary Model using thermo-mechanical properties can accurately predict the axial tensile behaviour and through-thickness thermal conductivity of a plain weave DLR-XT laminate;

(2) It's necessary to include waviness in the finite element models to accurately predict

the unit cell stress-strain response, and the composite through-thickness conductivity-strain response. A waviness angle of $\zeta = \pm 7^\circ$ has been used;

(3) For the plain weave DLR-XT composite, the degradation of transverse thermal conductivity is due to the wake debonding mechanism; in the future, the fibre/matrix interface air gaps are produced by a combination of shear strain will be investigated.

ACKNOWLEDGEMENTS

The authors gratefully acknowledge the financial support of the National Natural Science Foundation of China (11272207), and the Specialized Research Fund for the Doctoral Program of Higher Education (20120073120019).

REFERENCES

- [1] Marshall, D.B., Cox, B.N., Integral textile ceramic structures, *Annal Review of Materials Research*, 38, 2008, pp. 425-443.
- [2] Bernachy-Barbe, F., Gédart, L., Bornert, M., Crépin, J., Sauder, C., Anisotropic damage behavior of SiC/SiC composite tubes: Multiaxial testing and damage characterization., *Composites: Part A*, 76, 2015, pp. 281-288.
- [3] Pature, N.P., Advanced structural ceramics in aerospace propulsion, *Nature Materials* 15, 2016, pp.804-809.
- [4] Sheikh MA, Taylor SC, Hayhurst DR and Taylor R. Microstructural finite-element modelling of a ceramic matrix composite to predict experimental measurements of its macro thermal properties. *Modelling and Simulation in Materials Science and Engineering*, 2001, 9, pp. 7-23.
- [5] Del Puglia, P., Sheikh, M.A., Hayhurst, D.R., Classification and quantification of initial porosity in a CMC laminate, *Composites: Part A*, 35, 2004a , pp. 223-230.
- [6] Del Puglia, P., Sheikh, M.A., Hayhurst, D.R., Modelling the degradation of thermal transport in a CMC material due to three difference classes of porosity, *Modeling and Simulation in Materials Science and Engineering*, 12, 2004b, pp. 357-372.
- [7] Del Puglia, P., Sheikh, M.A., Hayhurst, D.R., Thermal transport property prediction of a CMC laminate from base material properties and manufacturing porosities, *Proceedings of the Royal Society A*, 461, 2005, pp. 3575-3597.
- [8] Sheikh MA, Hayhurst DR, Taylor SC and Taylor R., Experimental investigation of the effect of mechanical loading on thermal transport in ceramic matrix composites, *Journal of Multiscale Modelling*, 2009, 1, pp. 403-433.
- [9] Liu, D., Zheng, X., Wang, F., Liu, Y., Mechanism of thermomechanical coupling of high temperature heat pipe cooled C/C composite material thermal protection structure, *Acta Materiae Compositae Sinica*, 3(27), 2010, pp. 43-49.
- [10] Tang, C., Blacklock, M., Hayhurst, D.R., Uni-axial stress-strain response and thermal conductivity degradation of ceramic matrix composite fibre tows, *Proceedings of the Royal Society A*, 465, 2009, pp. 2849-2876.
- [11] Blacklock, M., Hayhurst, D.R., Multi-axial failure of ceramic matrix composite fiber tows, *Journal of Applied Mechanics*, 78, 2011, 031017-1 to 031017-10 (doi:10.1115/1.4002814).
- [12] Tang, C., Blacklock, M., Hayhurst, D.R., Stress-strain response and thermal conductivity degradation of ceramic matrix composite fibre tows in 0-90° uni-directional and woven composites, *Journal of Composite Materials*, 45 (14), 2010, pp. 1461-1482.
- [13] Cox, B.N., Carter, W., Fleck, N., A binary model of textile composites—I. Formulation, *Acta Metallurgica et Materialia*, 42, 1994, pp. 3463-3479.
- [14] Yang, Q.D., Cox, B.N., Spatially averaged local strains in textile composites via the binary model formulation, *Journal of Engineering Materials and Technology-Transaction of the ASME*, 125, 2003, pp. 418-425.
- [15] Yang, Q.D., Cox, B.N., Predicting failure in textile composites using the Binary Model with

- gauge-averaging. *Engineering Fracture Mechanics*, 77, 2010, pp. 3174-3189.
- [16] Blacklock, M., Hayhurst, D.R., Initial elastic properties of unidirectional ceramic matrix composite fiber tows. *Journal of Applied Mechanics*, 79, 2012, 051020-1 to 051020-11 (doi:10.1115/1.4005585).
- [17] SIMULIA. Abaqus user's manual, Version 6.12. Providence, Rhode Island, US. 2012.
- [18] Fourier, J., 1822. *Theorie Analytique de la Chaleur*. Firmin Didot. ISBN 9781108001809 (reissued by Cambridge University Press, 2009).
- [19] Zhang, D., Hayhurst, D.R., Stress-strain and fracture behaviour of 0°/90° and plain weave ceramic matrix composites from tow multi-axial properties, *International Journal of Solids and Structures*, 47, 2010, pp. 2958-2969 (doi: 10.1016/j.ijsolstr.2010.06.023).
- [20] Zhang, D., Hayhurst, D.R., Influence of applied in-plane strain transverse thermal conductivity of 0°/90° and plain weave ceramic matrix composites, *International Journal of Solids and Structures*, 48, 2011, pp. 828-842 (doi: 10.1016/j.ijsolstr.2010.11.017).
- [21] Zhang, D., Hayhurst, D.R., Effects of in-plane extension on transverse thermal conductivity of a carbon/carbon 8-harness satin weave composite, *International Journal of Damage Mechanics*, August 3, 2016 (doi: 10.1177/1056789516659332).